Hindawi Publishing Corporation
International Journal of Photoenergy
Volume 2011, Article ID 410352, 7 pages
doi:10.1155/2011/410352

Research Article

Influence of Parameters of Cold Isostatic Pressing on TiO_2 Films for Flexible Dye-Sensitized Solar Cells

Yong Peng,[1] Jefferson Zhe Liu,[2] Kun Wang,[1] and Yi-Bing Cheng[1]

[1] *Department of Materials Engineering, Monash University, Clayton, Melbourne, VIC 3800, Australia*
[2] *Department of Mechanical and Aerospace Engineering, Monash University, Clayton, Melbourne, VIC 3800, Australia*

Correspondence should be addressed to Yi-Bing Cheng, yibing.cheng@monash.edu

Received 22 February 2011; Accepted 9 May 2011

Academic Editor: Leonardo Palmisano

Cold Isostatic Pressing (CIP) is used to make TiO_2 working electrodes for flexible dye-sensitized solar cells (DSCs). Different CIP processes, varying pressures from 50 MPa to 200 MPa and holding time 1 s up to 600 s, are performed to study the effect of CIP on the resistivity of TiO_2 electrode thin films and the power conversion efficiency (PCE) of DSCs. The results show that the CIP process has significantly improved the PCE of DSC devices. Electrochemical impedance spectroscopy (EIS) analysis indicates a clear correlation between the PCE enhancement and the resistivity reduction in TiO_2 thin films after various CIP processes. Porosity reduction and localized joints formed between some TiO_2 nanoparticles due to the friction heat in the CIP process are believed to be responsible for the resistivity reduction of the TiO_2 working electrode thin films.

1. Introduction

Since dye-sensitized solar cell (DSC) was reported in 1991, it has been seen as a viable potential alternative to existing solar cell technologies [1, 2]. Due to its characteristics of being portable, of low costs, and high power conversion efficiency (PCE), flexible dye-sensitized solar cells have attracted interests of scientists and manufacturing industries in the last decade. However, the PCE of flexible DSCs has been relatively low because the plastic substrate cannot be sintered at high-temperature. The high temperature sintering, usually at ~500°C, benefits inter-TiO_2 particle connections and reduces internal resistance of TiO_2 working electrodes. Hence, in past years, many low-temperature processing methods were utilized to improve contacts between TiO_2 particles. Mechanical rolling and uniaxial pressing were such low-temperature techniques used to produce flexible working electrodes for DSCs [3, 4]. These techniques can improve the contacts between TiO_2 particles but would have some difficulty to achieve uniformity for large size devices.

Cold isostatic pressing (CIP) has been widely used as an effective pretreatment technique for compaction of ceramic and metal powders [5]. Compared with uniaxial pressing, samples compressed with CIP have higher relative density, better mechanical properties, and more even microstructures [6]. In some reports [7, 8], ceramic powders could be compressed to a maximum relative density of 70% after the CIP process. After being applied with high CIP pressure, nanoparticles can be sintered to a relative density of 99% or higher. Recent work by Weerasinghe et al. [9] has demonstrated CIP as an effective way to improve TiO_2 film quality for plastic-based DSCs. Systematic study of the CIP process on the properties of TiO_2 thin film and underlying mechanism, however, is still missing. Such knowledge is highly desired to optimize the CIP process for future DSC developments.

In this paper, we report a study on the compaction of TiO_2 nanoparticles in thin films subject to different CIP pressures and holding times. The photovoltaic and electrochemical impedance measurements show that the CIP process is an effective way for the improvement of the conversion efficiency of flexible DSCs due to the significant reduction of the electrical resistivity of the TiO_2 thin films. The possible reasons of resistivity reduction are also discussed in terms of porosity reduction of TiO_2 thin films and joints formed among TiO_2 nanoparticles caused by the friction heat in the CIP process.

2. Experimental

2.1. Cell Preparation. Working electrodes of DSCs are made of TiO_2 (P25, Degussa, Australia). First, TiO_2 nanoparticles were mixed with ethanol absolute to make a slurry with a TiO_2 content of about 30 wt% in a planetary ball mill [10] (Pulverisette 6, Fritsch). Then, the milled slurry was used to make films on ITO/PEN plastic substrates (13 Ω/□ , Peccell Technologies, Inc., Japan) via doctor blading. After being dried at 150°C for 30 min in air, films were compressed in a CIP machine (ABB Autoclave Systems, INC., USA). The applied pressure was 200 MPa, 100 MPa, and 50 MPa, and the holding time 1 s, 300 s, and 600 s, respectively. After being compressed, the films were used as working electrodes.

N719 dye, (Cis-bis(isothiocyanato) bis(2,2′-bipyridyl-4, 4′-dicarboxylato)-ruthenium(II)bis-terabutyl-ammonium (Solaronicx SA, Switzerland)), was used to sensitize working electrodes. Working electrodes were immersed into a dye solution with a content of 0.5 mM N719 dye in 1 : 1 ethanol and acetonitrile solution overnight. Sensitized working electrodes were then attached with a Pt|ITO|PEN counter electrode. After being filled with an electrolyte (0.04 MI_2, 0.4 M 4-tert-butylpyridine, 0.4 M LiI, 0.3 M N-methylbenzimidazole in 1 : 1 acetonitrile and 3-methoxypropionitrile solution), cells were prepared for tests.

2.2. Measurements. I-V characters of the cells were taken in an Oriel Solar Simulator system with monochromatic light by attaching a Pt|ITO|PEN to the dye-sensitized working electrodes under one sun for opening tests. The electrochemical impedance spectroscopy (EIS) of cells was taken in an electrochemistry station (Bio-Logic SAS). EIS spectra were recorded over a frequency range of 0.05–10^5 Hz under a lamp with a light density of 1 sun and adding a negative 0.6 V voltage to working electrodes. Resistance of cells was calculated via EC-Lab software (Bio-Logic SAS). The microstructures of the TiO_2 films were analyzed by using SEM (JEOL JSM 7001F) and TEM (Philips CM20). Film thickness measurements were taken via a Dektak 150 stylus profiler (Veeco Instruments Inc.).

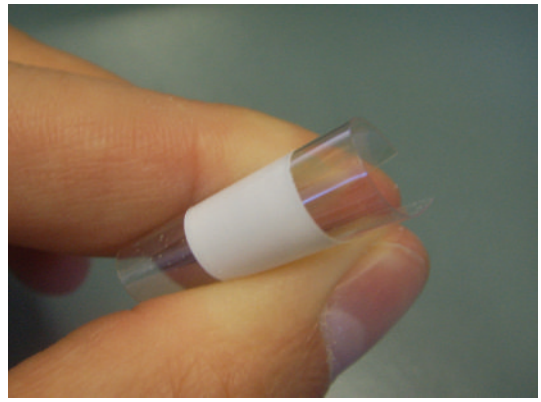

Figure 1: A Photo of a high-quality TiO_2 film produced by the CIP technique for flexible DSCs.

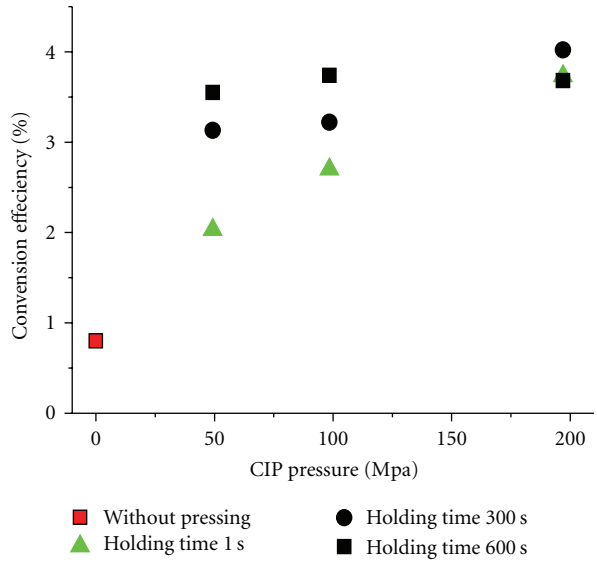

Figure 2: PCE of DSCs after the CIP process with pressure of 200 MPa, 100 MPa and 50 MPa and holding time of 1 s, 300 s, and 600 s, respectively. The PCE of the sample without CIP was 0.8%.

3. Results and Discussion

Figure 1 shows a high-quality TiO_2 film compressed with a CIP pressure of 200 MPa and holding time of 300 s. Figure 2 summarizes the PCE of the DSC devices after various CIP processes. In comparison to the PCE of the cells without CIP (0.8%), the improvement by the CIP process is significant. The highest PCE is obtained in the device compressed under a pressure of 200 MPa and holding time of 300 s. In most cases, the PCE of cells improves with the increase of both holding time and CIP pressure. The only exception is that under a pressure of 200 MPa, a holding time longer than 300 s leads to a slight decrease of PCE.

In our experiments, the only variable in the tested cells is the TiO_2 working electrode film. Hence, the enhancement of the PCE of the DSC cells can be attributed to the characteristic change of working electrodes under different CIP processes. Figure 3 shows SEM images of several TiO_2 films. Without CIP (Figure 3(a)), cracks can be observed in the TiO_2 film. Figures 3(b)–3(d) show that CIP compactions under pressure of 50 MPa, 100 MPa, and 200 MPa, respectively, have produced high-quality films without obvious cracks. Pressed at 100 MPa and 200 MPa, microstructures of crack sealing appear in the TiO_2 films. Figure 4 shows TEM images of the samples before and after the CIP process. Soft aggregation can be observed in the film before CIP (Figure 4(a)), and some interparticle joints can be found after the CIP compaction (Figures 4(b) and 4(c)).

Figure 5 shows the EIS analysis of the DSC cells. A schematic equal circuit of flexible DSCs is shown in Figure 6. The resistance R_h consists of the resistance of substrate, resistance between substrate and electrolyte, and resistance between substrate and TiO_2 film [11, 12], which are represented by R_s, R_{ITO}, and R_{CO} in Figure 6. R_1 is the resistance of the interface of electrolyte and counter

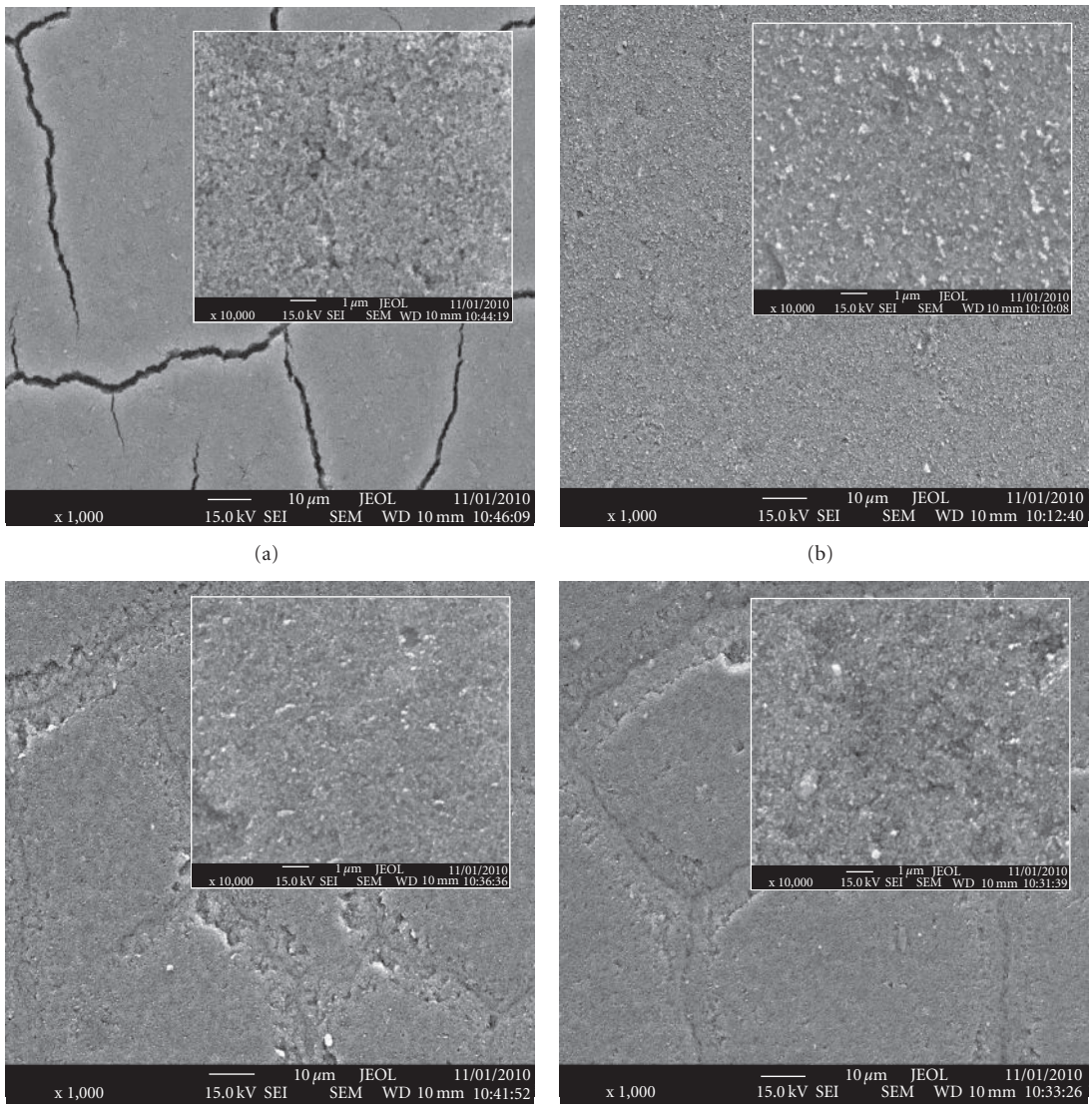

Figure 3: SEM pictures of films after various CIP processes. (a) film without CIP; (b) film with a CIP pressure of 50 MPa and holding time 1 s; (c) film with a CIP pressure of 100 MPa and holding time 600 s; (d) film with a CIP pressure of 200 MPa and holding time 600 s. The small inset shows the higher magnifications of each sample. The mark bar for the inset is 1 μm.

electrode represented by the semicircle in the EIS at the high-frequency band. Resistance R_2 represents transport resistance of electrons in TiO_2 films and the charge-transfer resistance of the charge recombination process between electrons in the TiO_2 film, dye and dye, I^-/I_3^- in the electrolyte, which are R_t and R_{ct}, respectively, in Figure 6. From Figure 5(b), it is very clear that R_h of the samples is significantly reduced by the CIP compaction, which can be attributed to the reduction of resistance between substrate and TiO_2 film. The overall internal resistance of a DSC device comprised of R_1, R_2, and R_h. According to Figure 5(d), the internal resistance decreased with the increase of CIP pressure up to 100 MPa and holding time up to 600 s, indicating that the electron transportation in these samples increased. However, an increase in the internal resistance of the device was found when the TiO_2 films had been compressed at 200 MPa for 600 s. Under this condition, there could be mechanical damage to the ITO coating on the PEN film. A lower internal resistance was recorded if the sample was pressed at 200 MPa but a shorter holding time.

It is well known that the CIP pressing leads to high relative density, good mechanical property, and uniform microstructures in ceramic films. Figure 7 depicts the thickness of TiO_2 electrode films after the CIP compaction. The original film thickness before the CIP pressing was around 8.2 μm. In our experiments, there was little change of the films in the lateral direction before and after the CIP pressing, thus the reduction of the film thickness is proportional to the increase of the packing density of nanoparticles. It is seen from Figure 7 that with increase of CIP pressure and holding time, the film thickness decreases gradually. At 200 MPa and a holding time of 600 s, the relative

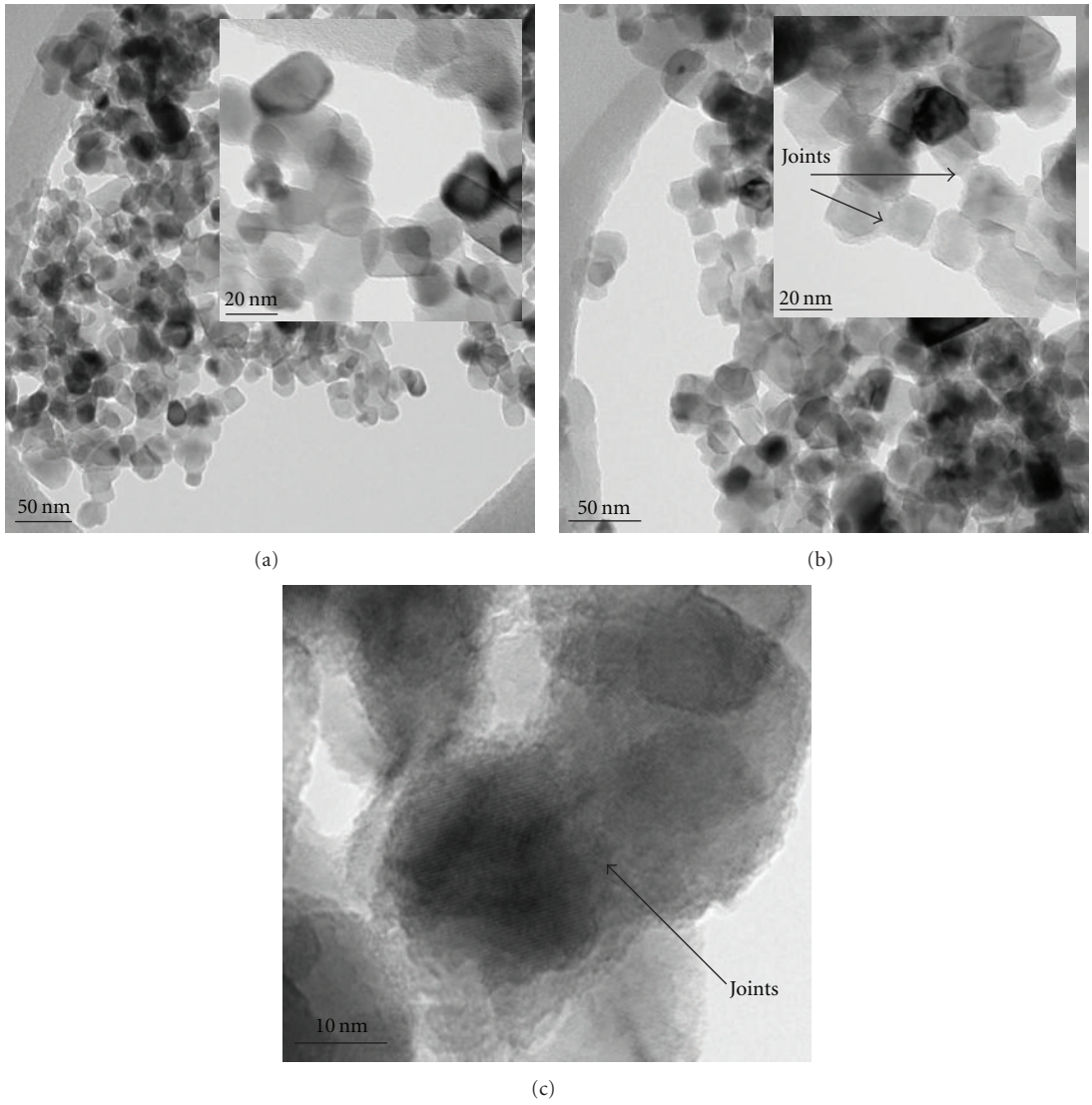

Figure 4: TEM images of TiO_2 films (a) without CIP and (b, c) with a CIP pressure of 200 MPa and holding time of 600 s. The small inset shows the higher magnification image of each sample.

packing density is increased to about 50%. Such an increase in packing density leads to the improved physical contacts between the nanoparticles and consequently the reduction of the resistivity, which can explain the observed reduction in resistivity (Figure 5) and improvement in the power conversion efficiency of the cells (Figure 2).

The improvement of the relative packing density of the TiO_2 film by the CIP compaction, however, cannot explain all the observed resistivity reduction and conversion efficiency improvement. In Figure 7, the samples pressed at 50 MPa, 100 MPa, and 200 MPa for one second, respectively, show a relatively small reduction in the film thickness compared to the one without CIP, but the reduction in resistivity (Figure 5) and the improvement in PCE (Figure 2) are quite significant. Moreover, the TiO_2 film prepared by CIP under 200 MPa for 1 s has lower resistivity and higher PCE than those pressed at 50 MPa for 300 s and 600 s (Figure 5), despite its packing density that is lower than the latter samples. It is assumed that the formation of the strong joints among TiO_2 particles may help explain these observations. Subjected to a high CIP pressure, the friction between TiO_2 nanoparticles would take place and thus convert the mechanical energy to thermal energy. The increased temperature would promote the atom diffusion among the nanoparticles, leading to the formation of interparticle chemical bonds. It is difficult to directly observe the formation of such chemical bonds in our experiments, thus a simple theoretical analysis is proposed. TiO_2 nanoparticles after the CIP process preserved its structural integrity (Figure 4). If the holding time is short, for example, several seconds, the heat flux out of the thin film can be assumed negligible. It suggests that the majority of the mechanical work is converted to thermal energy. The work done by the CIP is about $W = PA\Delta h$, where P is the CIP pressure being applied to films, A is the surface area of the think film, and Δh is the reduction of the film thickness. The increase of the thermo-energy is $U = \rho A h_0 C \Delta T$, where ρ is

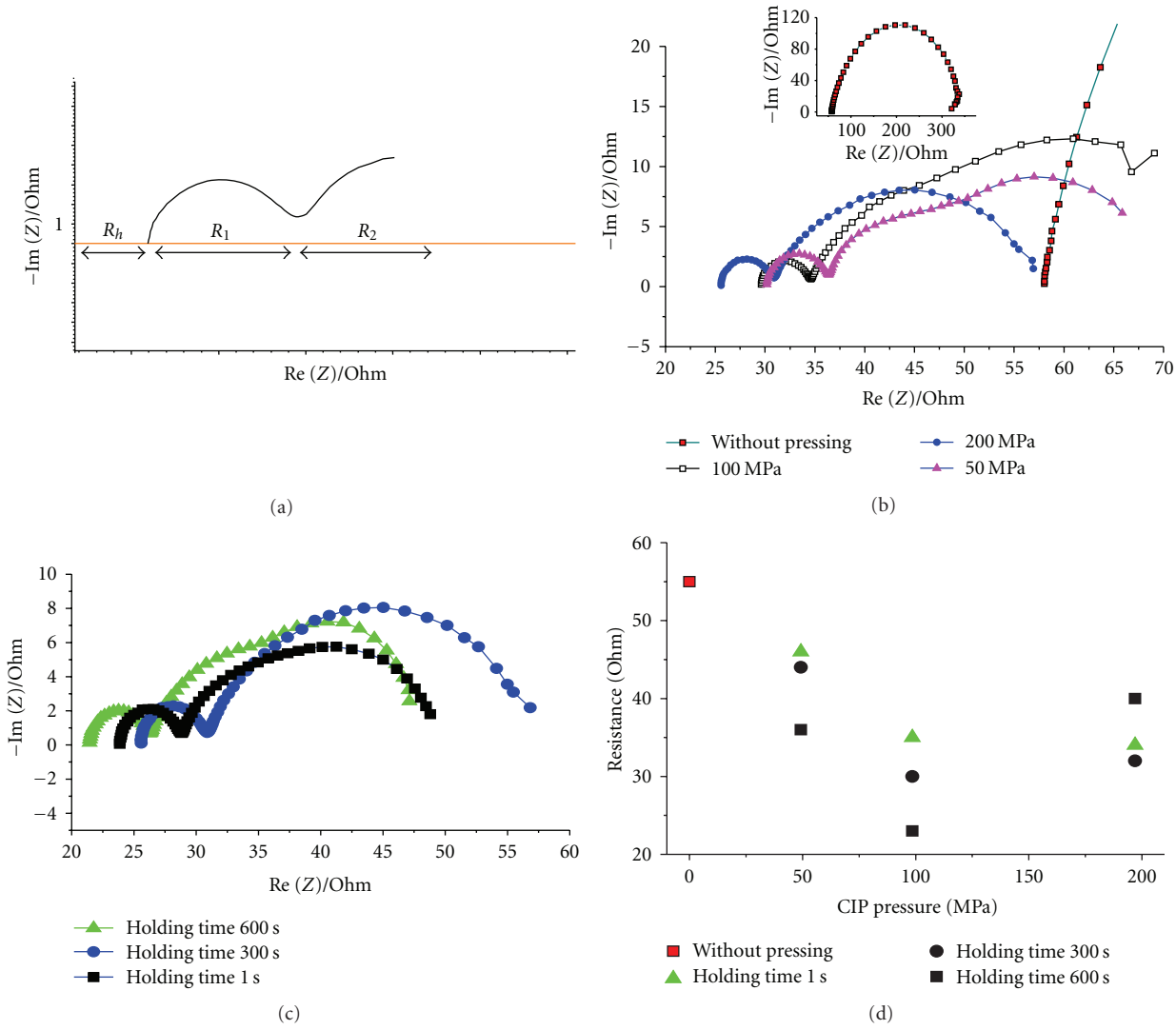

FIGURE 5: Nyquist impedance results of DSCs after various CIP processes. (a) Schematic diagram of the –Im(Z) versus Re(Z) curve; (b) Nyquist impedance results of samples without CIP and with CIP at different pressures for 300 s; (c) Nyquist impedance results of samples with the same CIP pressure of 200 MPa but different holding time; (d) calculated overall internal resistance of TiO_2 films after various CIP pressing. The overall internal resistance of the sample without pressing is 55 ohm.

the density of the TiO_2 nanoparticle film (average measured value is around 0.726 g/cm^3), h_0 is the thickness of the film before CIP, C is the heat capacity of TiO_2 film [13] (around 57 J/mol.k), and ΔT is the average temperature increase of the whole thin film. Thus, we have $\Delta T = P\Delta h/\rho h_0 C$. For a thin film pressed at CIP pressure 200 MPa and holding time 1 s, the estimated average temperature increase ΔT throughout the thin film is about 20 K. If we consider that the friction occurs at the contact points of the nanoparticles, the temperature increase at the contact points could be much higher than the ΔT *of the film*. For example, if we assume the TiO_2 nanoparticles of a diameter 20 nm (Figure 4) as a group of hexagonal close-packed balls subject to a 200 MPa pressure, according to Hertz contact model [14] between two elastic balls, the contact area is about 5% of the total surface. If all heat was produced as a result of interparticle friction, then the local temperature increase at the contact area could be one order of magnitude higher. In addition, it is well known that diffusion activation energy of atoms is lower at the nanoparticles interface/surface than in the bulk material. The high surface (interface)/volume ratio of the nanostructured materials thus leads to a higher diffusion coefficient than the corresponding bulk material [15–17]. Indeed, the formation of strong joints among gold nanoparticles has been observed when subjected to a sufficiently high pressure [18]. It is, therefore, possible that some chemical bonds would be formed due to the interparticle diffusion among the TiO_2 nanoparticles under the CIP pressing. The ΔT estimated for CIP pressures of 50 MPa and 100 MPa at a holding time 1 s are only about 1 K and 7 K, respectively. We can thus assume that there would mainly be physical contacts between the nanoparticles in these two

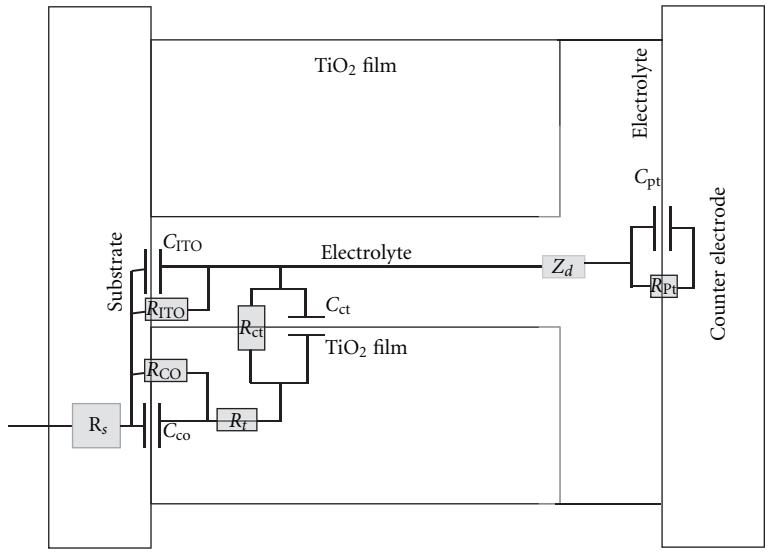

Figure 6: Equal circuit of DSC. R_{ct} is the charge-transfer resistance of the charge recombination process between electrons in the TiO_2 film and I_3^- in the electrolyte; R_t is the transport resistance of electrons in TiO_2 films; R_{ITO} is the charge-transfer resistance at exposed ITO/electrolyte interface; R_{co} is the contact resistance of ITO/TiO_2 interface; R_{pt} is the charge-transfer resistance of exposed Pt/electrolyte interface; C_{ct}, C_{ITO}, C_{co}, and C_{pt} are the chemical capacitance of the TiO_2 film, corresponding double-layer capacitance at the exposed ITO/electrolyte interface, capacitance at ITO/TiO_2 interface, and capacitor of Pt/electrolyte interface, respectively. R_s consists of the substrate resistance and series resistance between substrate and wires [11, 12].

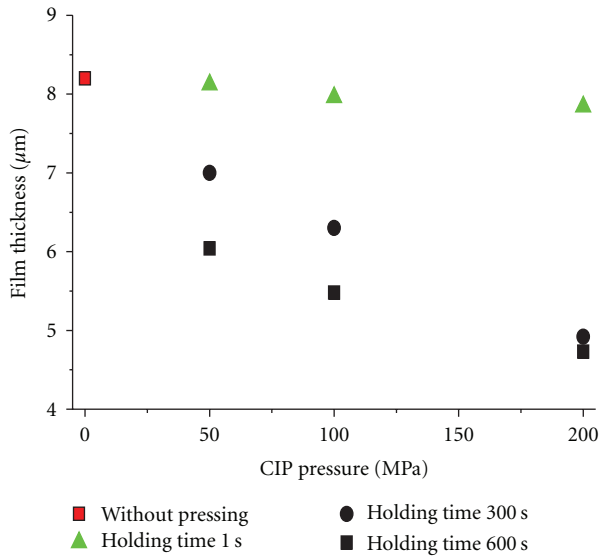

Figure 7: TiO_2 film thicknesses after CIP compressing at different conditions; the film thickness before CIP pressing was 8.2 μm.

cases. At CIP pressure 50 MPa and holding times 300 s and 600 s, the film thickness further reduced and the estimated average temperature increases ΔT would be about 14 K and 25 K, respectively. They are close to the estimated value for CIP pressure 200 MPa and holding time 1 s. Since the holding time in these two cases is much longer, the heat flux out of the electrode thin film could significantly lower the estimated temperature. This explains the relatively lower PCE in these two samples.

4. Conclusions

In this paper, the effects of the CIP technique on the improvement of conversion efficiency of DSCs have been studied with the CIP pressure varying from 50 MPa to 200 MPa and holding time from 1 s to 600 s. Our results show a general trend that with the increase of the pressure and holding time, the resistivity of the TiO_2 thin film electrode decreases and the PCE improves. At pressure 200 MPa, holding time longer than 300 s does not lead to a significant efficiency improvement, which may be attributed to the mechanical damage to the ITO coating on the PEN film. The effects of the CIP pressure on the efficiency of DSCs on plastic substrates could be related to the improvement of the packing density of TiO_2 films and the possible formation of chemical bonds among the nanoparticles.

Acknowledgment

Support from the Victorian Organic Solar Cell Consortium (VICOSC) is greatly appreciated by the authors.

References

[1] M. Gratzel, "Recent advances in sensitized mesoscopic solar cells," *Accounts of Chemical Research*, vol. 42, no. 11, pp. 1788–1798, 2009.

[2] L. M. Gonçalves, V. de Zea Bermudez, H. A. Ribeiro, and A. M. Mendes, "Dye-sensitized solar cells: a safe bet for the future," *Energy & Environmental Science*, vol. 1, no. 6, pp. 655–667, 2008.

[3] H. Lindstrom, A. Holmberg, E. Magnusson, S.-E. Lindquist, L. Malmqvist, and A. Hagfeldt, "A new method for manufacturing nanostructured electrodes on plastic substrates," *Nano Letters*, vol. 1, no. 2, pp. 97–100, 2001.

[4] T. Yamaguchi, N. Tobe, D. Matsumoto, and H. Arakawa, "Highly efficient plastic substrate dye-sensitized solar cells using a compression method for preparation of TiO_2 photoelectrodes," *Chemical Communications*, no. 45, pp. 4767–4769, 2007.

[5] I. M. Robertson and G. B. Schaffer, "Review of densification of titanium based powder systems in press and sinter processing," *Powder Metallurgy*, vol. 53, no. 2, pp. 146–162, 2010.

[6] M. Trunec and K. Maca, "Compaction and pressureless sintering of zirconia nanoparticles," *Journal of the American Ceramic Society*, vol. 90, no. 9, pp. 2735–2740, 2007.

[7] I.-W. Chen and X.-H. Wang, "Sintering dense nanocrystalline ceramics without final-stage grain growth," *Nature*, vol. 404, no. 6774, pp. 168–171, 2000.

[8] K. T. Kim, S. C. Lee, and H. S. Ryu, "Densification behavior of aluminum alloy powder mixed with zirconia powder inclusion under cold compaction," *Materials Science & Engineering A*, vol. 340, no. 1-2, pp. 41–48, 2003.

[9] H. C. Weerasinghe, P. M. Sirimanne, G. P. Simon, and Y.-B. Cheng, "Cold isostatic pressing technique for producing highly efficient flexible dye sensitized solar cells on plastic substrates," *Journal of Progress in Photovoltaics*. In press.

[10] H. C. Weerasinghe, P. M. Sirimanne, G. P. Simon, and Y.-B. Cheng, "Fabrication of efficient solar cells on plastic substrates using binder-free ball milled titania slurries," *Journal of Photochemistry & Photobiology A*, vol. 206, no. 1, pp. 64–70, 2009.

[11] Q. Wang, S. Ito, M. Gratzel et al., "Characteristics of high efficiency dye-sensitized solar cells," *Journal of Physical Chemistry B*, vol. 110, no. 50, pp. 25210–25221, 2006.

[12] L. Y. Han, N. Koide, Y. Chiba, A. Islam, and T. Mitate, "Modeling of an equivalent circuit for dye-sensitized solar cells: improvement of efficiency of dye-sensitized solar cells by reducing internal resistance," *Comptes Rendus Chimie*, vol. 9, no. 5-6, pp. 645–651, 2006.

[13] D. de Ligny, P. Richet, E. F. Westrum Jr., and J. Roux, "Heat capacity and entropy of rutile (TiO2) and nepheline (NaAlSiO4)," *Physics and Chemistry of Minerals*, vol. 29, no. 4, pp. 267–272, 2002.

[14] S. P. Timonshenko and J. N. Goodier, *Theory of Elasticity*, McGraw-Hill, New York, NY, USA, 1970.

[15] M. R. Ranade, A. Navrotsky, H. Z. Zhang et al., "Energetics of nanocrystalline TiO_2," *Proceedings of the National Academy of Sciences of the United States of America*, vol. 99, no. 2, pp. 6476–6481, 2002.

[16] A. A. Levchenko, G. Li, J. Boerio-Goates, B. F. Woodfield, and A. Navrotsky, "TiO_2 stability landscape: polymorphism, surface energy, and bound water energetics," *Chemistry of Materials*, vol. 18, no. 26, pp. 6324–6332, 2006.

[17] S.-M. Lee, D. G. Cahill, and T. H. Allen, "Thermal conductivity of sputtered oxide films," *Physical Review B*, vol. 52, no. 1, pp. 253–257, 1995.

[18] Q. Jiang, S. H. Zhang, and J. C. Li, "Grain size-dependent diffusion activation energy in nanomaterials," *Solid State Communications*, vol. 130, no. 9, pp. 581–584, 2004.